Generation of the coherent pulses by the CDW-motion. Solutions of the microscopic model equations

I. Batistić, A. Bjeliš, L.P. Gor'Kov

J. Physique **45** (1984) 1049-1059 JUIN **1984,** PAGE 1049

Classification
Physics Abstracts
72.15N — 72.20H

Generation of the coherent pulses by the CDW-motion. Solutions of the microscopic model equations

I. Batistić (*), A. Bjeliš (*) and L. P. Gor'kov (**)

(*) Institute of Physics of the University, POB 304, 41001 Zagreb, Croatia, Yugoslavia
(**) L. D. Landau Institute for Theoretical Physics, ul. Kosygina 2, Moscow 117 940, USSR

(*Reçu le 3 janvier 1984, accepté le 16 février 1984*)

Résumé. — Le transport collectif par les ondes de densité de charge (CDW) se transforme en un courant ordinaire dans les contacts avec le métal normal. Dans notre étude ce processus se produit par le glissement de phase (PS) de CDW. Le CDW dans un système quasi unidimensionnel avec une surface de Fermi à « nesting » et en présence d'impuretés est décrit par une équation différentielle non linéaire obtenue auparavant. Nous résolvons cette équation numériquement pour des échantillons semi-infinis et finis. L'analyse des solutions est faite pour des champs électriques E et les longueurs d'échantillon L qui sont respectivement d'un à deux ordres de grandeur plus grands et petits que les valeurs expérimentales actuelles. Il s'ensuit que les solutions PS sont fonctions du temps à une période, avec la distance du centre PS au contact variant comme $E^{-0,284}$ dans la limite des petits champs. Le transport cohérent par CDW existe au-dessus d'un champ de seuil qui varie comme $L^{-1,23}$. Nous avons examiné aussi les pulses dans le voltage, produits par le processus de PS. Les résultats sont en bon accord avec la dépendance en longueur des champs de seuil et certaines propriétés de bruit périodique, observés dans $NbSe_3$ et TaS_3.

Abstract. — The collective transport of charge density waves (CDW) converts into an ordinary current at the contacts with a normal metal. In the present work this conversion is proposed to proceed *via* the process of phase slippage (PS). The CDW in the quasi-one-dimensional system with a nested Fermi surface and impurities is described by the nonlinear differential equation derived earlier. This equation is solved numerically for semi-infinite samples, as well as for finite samples with both edges fixed. The analysis of solutions is carried out for electrical fields E and sample lengths L which are respectively one to two orders of magnitude larger and smaller than the actual experimental values. This leads to the following results : the PS solutions are one-periodic functions of time, with the distance of the PS centre from the fixed end behaving like $E^{-0.284}$ in the limit of small E. The coherent CDW transport in the finite samples occurs above the threshold field which varies as $L^{-1.23}$. The pulses in the voltage generated by PS processes are also analysed. The results are in a good agreement with the experimental data for the length dependence of the threshold field and with some properties of the periodic noise in e.g. $NbSe_3$ and TaS_3.

1. Introduction.

The investigations in the trichalcogenide transition metal compounds like $NbSe_3$ and TaS_3 are now mostly concentrated on the so-called Fröhlich conductivity mechanism and the problem of the narrow band « noise » generation produced, speaking in general terms, by the charge density wave (CDW) motion as it has first been proposed (Refs. [1-3]). For the more extensive list of references and the comprehensive discussion of the whole problem see, for instance, reference [4]. Many theories have been developed since that time suggesting both microscopical and phenomenological approaches to explain the phenomena observed. All of them have met difficulties in attempting to explain the very narrow, almost coherent character [2] of the voltage oscillations generated in the sample in the presence of a passing current, when the average applied field, E, exceeds E_t, the threshold electric field, for the CDW motion. Recently it has been discovered experimentally that these oscillations have the local origin and are positioned near the measuring contacts where the current carried by the collective CDW motion converts into the ordinary transport current [5-7]. The intuitive picture suggested in references [6, 7] is, roughly speaking, as follows. There is a surface near the contact defined by the condition that the local electric field $E(r)$ (the distribution of currents and fields gets inhomogeneous near the contact) equals to the threshold value

$$E(r) = E_t .$$

At this surface the CDW motion stops and the asso-

ciated phase undergoes a sort of phase-slip process. The picture of that process involves an *ad hoc* coherent motion of vortices moving along the surface mentioned above, and synchronizing each other strongly to preserve the periodical character of oscillations. The phenomenological equation for this behavior has been borrowed from the Josephson junction theory.

Independently, another model has been proposed by one of the authors [8] in the framework of a 3D microscopical model. The intention was to separate such a phenomenon as is the finite threshold field, E_{tb}, which is due to the bulk pinning effects by impurities, from the generation of oscillations at the interface with the ordinary metal. The stoppage of the CDW phase transport in the vicinity of the contacts and its conversion into the normal current, inevitably goes together with the successive disappearance of CDW wavelengths in time. With the lattice deformations at the interface being fixed, this is realised through the formation of the centers at which the CDW amplitude vanishes and the overall phase difference in space changes by 2 π. The aim of the microscopical model [8] is to describe explicitly this process called the phase slippage, and to prove the existence of the nonlinear periodic regime. Then, if it so happens that the phase slip (PS) occurs at a distance from the interface large enough not to feel the roughness of the real contact and to avoid any pinning, this would lead to the coherent (periodic) oscillation in the system. Such model can be called « sample quality independent », and is to be applied for samples of the good quality with the low enough threshold field E_{tb} and the large room resistance ratio. The nature of the surface energy which is connected with the interface and stops the CDW phase transport, lies in the fact that even at $T > T_p$ (T_p, the structural transition temperature) there are equilibrium atomic displacements from the regular lattice due to the boundary separating the two metals. These displacements of the lattice are weakly affected by the onset of the new (Peierls) state in one of the two metals at $T < T_p$. Therefore, the superstructure which grows in the lattice below T_p, is to match the « tail » of the boundary effects at the characteristic scale of order $\xi_0 \sim \hbar v_F/T_p$ from the border. Taking $v_F \simeq 10^7$ cm/s, $T_p \simeq 50$ K (as for lower transition on $NbSe_3$), one gets $\xi_0 \simeq 10^{-6}$ cm. In order to introduce the homogeneous effective boundary conditions (i.e. to forget about the roughness of the real interface) it is necessary for the phase-slippage process to occur on distances larger than ξ_0. If it is so, the system of the nonlinear equations with the appropriate homogeneous boundary conditions will immediately give nonlinear periodic regime, or the so-called « cycle » at any specific geometry of the real contact interface. (We put aside the small amount of defects which seems to be the only source of finite width of the harmonics in this case.) We shall show that this picture really works in the limit of sufficiently weak electric fields, as it takes place in the available experimental situations.

The paper is organized as follows. In section 2 we give a short account of the underlying microscopic model [8, 9], and formulate the problem of the CDW motion in the vicinity of interfaces with a normal metal. The results of the numerical analysis of this problem are presented in section 3. In section 3.1 we simulate numerically the time evolution of the Fröhlich mode in the finite sample, while in section 3.2 we consider PSs in a semi-infinite sample with one free end. The properties of periodic voltage induced by PS processes are discussed in section 3.3. Finally, in the concluding section 4 we make a preliminary comparison with some known experimental data.

2. The model and the formulation of the problem.

In this section we recall shortly the main features of the model [7]. In this model it is assumed that the electron Fermi surface consists of two separate sheets : the first on the right, the second on the left side of the Brillouin zone (the chain direction is taken as the x-axis). These sheets are of the three dimensional character even with respect to the perpendicular transport (to avoid the unessential complications in the quasi-one-dimensional (Q1D) case) and possess the « nesting » property $\varepsilon(\mathbf{K}) = -\varepsilon(\mathbf{K} + \mathbf{Q})$ (where $\mathbf{Q}$ is the 3D « nesting » vector). This type of spectrum appears, for example, in the tight-binding approximation for the so-called one chain compounds [10]. The topological properties which permit to map the more realistic energy spectrum of the Q1D materials into this model are, firstly, that the Fermi surfaces are open in the perpendicular direction and, secondly, that the longitudinal component of the « nesting » vector $Q_{\parallel} = 2 K_F$ is incommensurate with the underlaying lattice. The model with an exact nesting permits the rigorous mathematical treatment [11], in many aspects resembling the formalism of the BCS-theory. In order to obtain the simplest form of equations for the order parameter

$$\Delta = |\Delta| \exp(i\phi) \tag{1}$$

which determines the gap in the electron spectrum of the new phase produced by the spontaneous structural (Peierls) deformation, this model has been simplified using the limit in which impurities suppress the transition temperature : T_p goes to zero at the finite concentration of defects exactly in the same way as it takes place for the paramagnetic impurities in the superconductivity (by smoothing the singularity in the density of states of new phase at zero temperature). This has made possible to derive the time dependent version of the Landau-type expansion in the magnitude of the order parameter (1) in the region close to the critical concentration, $T_p \ll T_{p0}$ (T_{p0} the Peierls transition temperature of the model in absence of impurities). The procedure of the derivation of the corresponding equations is described in reference [9]

(see also Ref. [8]). Before writing down these equations let us remind that the gap parameter is connected with the lattice distortion

$$u(\mathbf{r}) = u_0 \cos(\mathbf{Q}\mathbf{r} + \phi)$$

by the relation $| \Delta | = \frac{d}{2} u_0$ where d is the deformational potential. The phase ϕ reflects the possibility of motion for the CDW in the incommensurate case. It is also worth mentioning that because of the explicit assumption concerning the 3D character of the Fermi surface the threshold electric field E_{tb} in this model can be made negligibly small.

The resulting equations obtained in references [8, 9] have the form

$$\dot{\Delta} + iE\Delta - \Delta + |\Delta|^2 \Delta - \nabla^2 \Delta = 0 . \qquad (2)$$

The parameters in equation (2) are dimensionless. Thus, E is measured in terms of $\pi^2 T_p^2 \delta / 6 \bar{v}_x e$ and $|\Delta|$ in terms of $|\Delta_\infty|$ ($|\Delta_\infty|^2 = \frac{6}{5} \pi^2 T_p^2 \delta$) where $\bar{v}_x$ is the mean longitudinal electron velocity, and $\delta = 1 - T^2/T_p^2$. (Note that here δ can be of order of unity.) The time and space scales are respectively defined by ω_0^{-1} and $\xi_{\parallel,\perp}$. The frequency ω_0 is given by

$$\omega_0 = \frac{4\pi^2}{9} T_p^2 \tau_c \delta ,$$

where $\tau_c = \frac{4\gamma}{3\pi T_p^0}$ (γ, Euler constant) for the concentration of defects close to its critical value ($T_p \ll T_{p0}$). $\xi_\parallel$ and $\xi_\perp$ are the coherence lengths in the longitudinal and transverse directions respectively,

$$\xi_{\parallel,\perp}^2 = \frac{27 \kappa_{\parallel,\perp}^2}{2\pi^2 T_p^2 \delta},$$

with

$$\kappa_\parallel^2 = \overline{v_x^2}\left[\ln\left(\frac{3}{2}\right) - \frac{1}{3} - \frac{\bar{v}_x^2}{\overline{v_x^2}}\left(\ln\left(\frac{3}{2}\right) - \frac{7}{8}\right)\right]$$

and

$$\kappa_\perp^2 = \overline{v_x^2}\left[\ln\left(\frac{3}{2}\right) - \frac{1}{3}\right].$$

For $T_p \ll T_{p0}$ the current j is obviously mainly due to the normal carriers

$$j = \frac{\sigma_n \pi^2 T_p^2 \delta}{6 \bar{v}_x e}\left[E - \lambda E |\Delta|^2 - \frac{8}{9} \varepsilon \lambda |\Delta|^2 \dot{\phi}\right]. \qquad (3)$$

The second and third terms are small corrections respectively due to the small decrease in a number of carriers and to the CDW motion ($\varepsilon \equiv \bar{v}_x^2 / \overline{v_x^2}$). The measure of smallness of these contributions is given by

$$\lambda = \frac{16\pi^2}{5}(T_p \tau_c)^2 \delta \ll 1 \qquad (4)$$

since $T_p \ll T_{p0}$ near the critical defect concentration in this model.

The expansion (3) for the current density presents an important formal simplification : at a given current the field E is defined by the normal conductivity and should be considered as an external parameter in equation (2). By solving equation (2) it is then possible to find the electric voltage (or current) corrections from the small terms in (3), considering them as perturbations in (2).

The problem of boundary conditions for $|\Delta| e^{i\phi}$ has been discussed in reference [9]. The appropriate boundary conditions for the planar interface imply that the gradient of phase normal to the plane gets zero at $x \to 0$, while the amplitude $|\Delta(x)|$ increases sharply to match the displacements of the atoms at the contact which are of the order of lattice constant. From the point of view of numerical calculations this choice would considerably complicate the calculation procedure. Therefore, in what follows we use the condition that the phase of the order parameter in (1) is fixed at the border ($\phi_0 = 0$) keeping the value of its amplitude at the interface, $|\Delta_0|$, different from unity, i.e. $|\Delta_0|$ can exceed the thermodynamical value of $|\Delta|$ at infinity (i.e. very far from the contact).

The next point is that, as we shall see, there are reasons to expect that the phase slippage takes place at distances considerably larger than $\xi_0 (x_{ps} > 1)$ if the electric field is weak enough. The obvious physical definition of the « strong field » is that the energy acquired by electron on distances of order of ξ_0, $eE\xi_0$ is large enough to remove it from the condensate (i.e. to put it across the gap $2|\Delta| \sim T_p$). From this point of view the electric fields used in the experiment ($E \sim 100$ mV/cm) are extremely small i.e. of the order $eE\xi_0/T_p \sim 10^{-4}$ in our dimensionless notations. We shall therefore pay special attention to the low electric field regime. If it so and x_{ps} is large, the geometry of contact will not be essential and the phase slip processes take place in the plane $x = x_{ps}$ perpendicular to the main conducting axis.

In the present work we limited our calculations to the planar situation when all the quantities depend on one space coordinate, x, only. Strictly speaking, this approach would be exact if the thickness of sample is small. For the thick enough sample the motion of dislocation in the superlattice (with the new wave vector $\mathbf{Q}$) is possible as it has already been mentioned above. However, the sample surface as a barrier for the penetration of dislocations, and especially the existence of the strand domains [12], make it possible that the solution with $\Delta(x, t) = 0$ in the whole plane $x = x_{ps}$, can have a wider range of applicability. In any case, the planar solution demonstrates the main features of the phase slippage phenomena and suggests an estimate for the position of x_{ps}.

Any crude analytical estimation of x_{ps} as a function of E is not reliable since actually we have to find the limiting cycle of the system of nonlinear equations (2). However, for the better orientation in the problem and in order to demonstrate the main physical mecha-

nisms involved we shall briefly enumerate various possibilities.

Let us rewritte (2) in the form in which the absolute value of Δ and its phase are independent variables [8],

$$\dot{|\Delta|} - |\Delta| + |\Delta|^3 - Q^2 |\Delta| - |\Delta|_{xx} = 0 \quad (E + \dot{\phi}) |\Delta|^2 - \frac{\partial}{\partial x}(|\Delta|^2 Q) = 0 , \tag{5}$$

and where $Q \equiv \partial\phi/\partial x$. Near the interface there is no CDW motion and at $E \ll 1$ one would obtain the following solution in this region

$$|\Delta|^2 = 1 - Q^2 , \qquad 3Q - \operatorname{Arctanh} Q \approx Ex . \tag{6}$$

This shows that the phase gradient Q grows up with x, diminishing the gap magnitude and destabilizing locally the Peierls state. This merely means that the electric field violates the local « nesting » conditions involved in the definition of the order parameter (1).

The mechanism (6) would correspond to the PS-regime at

$$x_{ps} \sim 1/E . \tag{7}$$

On the other hand, at small x, Q increases as

$$|Q| = |E| x .$$

This corresponds to the additional contribution into the gradient squared term of the free energy expansion $Q^2 |\Delta|^2$. Integrating over x (from $x = 0$, to $x = x_{ps}$) one gets the total energy loss due to increase of Q :

$$E^2 x_{ps}^3 .$$

We can compare this energy with the energy needed for the formation of a sort of a « kink », i.e. of a segment in which $|\Delta|$ sharply changes and goes down having a minimum on the unit (i.e. ξ_0) scale. The corresponding energy of this « kink » is of the order of unity (in our dimensionless variables). Therefore, this shows that the state with the growing gradient gets metastable already at a distance

$$x_{ps} \sim E^{-2/3} \, (Q^2 = E^{2/3} \ll 1) . \tag{8}$$

Suppose that this strong perturbation is somehow created, making the beginning to the further development of the phase-slip process. However, this position is yet not well defined with respect to the boundary. The establishing of the final location for the phase-slip process is due to some effective interaction with the interface to synchronize the phase-slippage with the phase transport due to the CDW motion at infinity. This feed-back interaction can be, of course, quite nonlinear, but in the linear approximation our equations correspond to the thermoconductivity (parabolic) equation for the phase. If we then assume that the phase jump $[\delta\phi] = 2\pi$ reaches the boundary and comes back during the single period $2\pi/E$ in the process of linear diffusion, the position of x_{ps} can be expected at

$$x_{ps} \sim E^{-1/2} . \tag{9}$$

So far, (9) gives the most severe restrictive condition on the distance x_{ps} comparing with the other possibilities (Eqs. (7) and (8)). One should mention however that the feed-back mechanism which fixes x_{ps} can be strongly nonlinear, and our numerical results point out in this direction.

We shall finish this section by the comment that the phase slip concept immediately leads to the appearance of the finite threshold field values for the finite length samples even for the perfect material. In a large enough sample the phase slips occur near both ends of the sample with the CDW moving in between. In short sample there is simply « no room » for the CDW motion to take place at a given electric field.

3. Results of numerical calculations.

We already stressed that the relevant experimental values of external electric field are very small ($E \ll 1$ in our dimensionless notations). This is just the range of fields for which the appearance of PSs in the close vicinity of the contacts with a normal metal is accounted for in the most reliable way by the model considered here. However, the above discussion indicates that the processes responsible for the formation of PS are essentially of the nonlinear nature. This is particularly so for $E \ll 1$, when the linearized approach leads to the quite extended region in the x-space which is unstable, so that a more rigorous treatment of (2) is required. It is therefore necessary to undertake the numerical analysis of the problem (2), i.e. of the coupled pair of differential equations for the real and imaginary parts (Δ_1 and Δ_2) of the order parameter Δ. (Note that the pair of equations for $|\Delta|$ and ϕ (5) is not very convenient for the numerical integration due to the singularity in the equation for ϕ in the slippage ($|\Delta| \approx 0$) regions).

In our numerical analysis we considered two situations which have some common points. Firstly, we calculated the space and time variations of a CDW in the sample of finite length L. The contacts at both ends are modelled as effective boundary conditions due to which the amplitude and the phase of CDW remain fixed at $x = 0$ and $x = L$, and vary gradually towards the interior of the sample. Our aim was to follow the appearance of PSs inside the sample and to determine the threshold field E_T as a function of L and of effective boundary conditions. Secondly we simulated a semi-infinite system. In that case CDW is taken to be fixed at the contact ($x = 0$), while far enough from the contact ($x \to \infty$) it acquires the simple translational solution

$$|\Delta| = 1 , \qquad \phi = Et \tag{10}$$

of (2). Under such boundary conditions the CDW has to experience PSs at some distance $x_{ps}(t)$. We took the right end L_∞ (« $x = \infty$ ») to be far enough ($L_\infty \gg x_{ps}$) and imposed the boundary condition (10) at $x = L_\infty$. Having checked that the finiteness of L_∞ does not influence the slippage region $x \approx x_{ps}$, we determined the position x_{ps} as a function of E, and for a given boundary condition at $x = 0$.

Other important information concerns the way in which a CDW evolves between two successive slippages. Knowing $\Delta(x, t)$, we are able to determine the time dependent voltage originating from PSs. The relevant quantity is the internal electric field in (3) :

$$\delta E(x, t) = \lambda E \mid \Delta \mid^2 + \frac{8}{9} \lambda \varepsilon \mid \Delta \mid^2 \dot{\phi} . \qquad (11)$$

It is convenient to measure this field with respect to its value averaged over a time period ($\langle \ \rangle_t$) :

$$\delta' E(x_1 t) = \delta E(x, t) - \langle \delta E(x, t) \rangle_t . \qquad (12)$$

The corresponding voltage between two end contacts (or across the slippage region in the case of semi-infinitive sample) is then

$$V(t) = \int_0^{L (\text{or } L_\infty)} \delta' E(x, t) \, dx . \qquad (13)$$

The properties of this voltage in the two situations listed above will be discussed at the end of this section.

We calculated numerically the solutions of (2) for samples with lengths L up to 100, while L_∞ in semi-infinite samples was taken between 10 and 30, depending on the value of E. The x-scale was usually divided into 100 points (200 for larger values of L). We used an inhomogeneous division of the x-scale, with the density of discrete x-points chosen to be largest in PS ranges. Still, the discreteness of x-scale was the main source of the numerical imprecisions, which were kept below about 1 % in all results for $\Delta(x, t)$ to be presented.

3.1 FINITE SAMPLES. — Let us assume that the CDW is constant all over the sample of the length L,

$$\Delta_1 = 1 , \qquad \Delta_2 = 0 , \qquad (14)$$

and that it is not able to vary at its edges $x = 0$ and $x = L$. At $t = 0$ we switch on instantaneously the constant electric field E. How will the CDW evolve in later times ?

The numerical simulation of this experiment gives the following overall answer. For electrical fields stronger than some threshold field $E_T(L)$, the CDW passes periodically in time through PSs which occur simultaneously and are positioned symmetrically at distances $x_{ps}(E)$ and $L - x_{ps}(E)$. The periodic behaviour

$$\Delta(x, t + t_p) = \Delta(x, t)$$

is achieved quite fastly after switching the electrical field (usually in a lapse of time shorter than t_p). For $E < E_T(L)$ the behaviour of the CDW is completely different. It tends to a stationary (time independent) state, approaching it either gradually, or through damped oscillations (for $E_T(L) - E$ small enough).

The dependence of the threshold field on the sample length is presented in figure 1. Already for $L \gtrsim 15$, it is well described by the power law

$$E_T(L) \simeq 2.55 \, L^{-\alpha} \qquad (15)$$

with $\alpha = 1.23 \pm 0.05$.

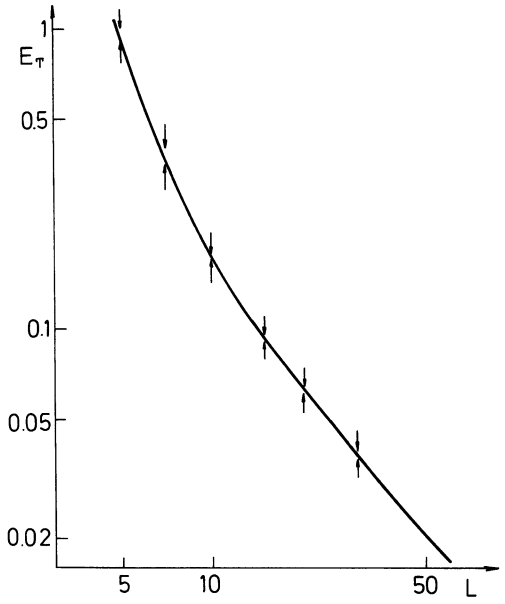

Fig. 1. — The threshold field as a function of the sample length. The arrows indicate the extreme points reached numerically from both sides of threshold.

The bending of the curve $E_T(L)$ in the range $L \lesssim 15$ is to be attributed to the interference between the two slippage centres which are closer and closer to one another as L decreases. On the other hand, the fact that the ratio $x_{ps}/(L/2)$ fastly decreases as L increases (Fig. 2) suggests that the law (15) is already asymp-

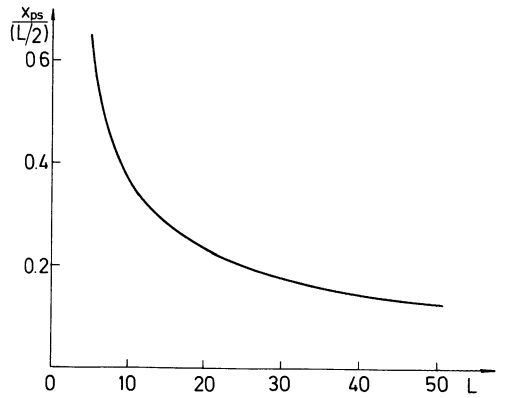

Fig. 2. — The ratio $x_{ps}/(L/2)$ *versus* the sample length L.

totic, and that it can be extrapolated to the limit $L \to \infty$. More precisely, this law should cover the small lengths for which $E_T(L)$ exceeds E_{tb}. For larger values of L the finiteness of the sample ceases to be relevant for the threshold field. In considering the length dependence we note that the samples for which the effect of the finite length on the threshold field is observed, are at least one to two orders of magnitude longer ($L \gtrsim 10^2$-10^3 in our units) than those of figure 1. We therefore proceed by considering mainly our « asymptotic » limit (15) of large values of L.

The further interesting point is the behaviour of the CDW on both sides of the threshold field, especially in the slippage range $E - E_T(L) \geqslant 0$. As E increases, two PSs shift towards the sample edges. Since their mutual distance increases, the interference effects weaken then. Indeed, the dependence of x_{ps} on E is indistinguishable from that obtained for a semi-infinite system (see Sect. 3.2 and Fig. 7).

The most direct evidence that two PSs do not overlap significantly comes from the evolution of one PS in time. For $L = 10$ and $E - E_T \simeq 0.0028$ ($E_T(10) \simeq 0.1722$) this is shown in figure 3, which contains the time dependence of the minima of the CDW amplitude, Δ_{min}, and of the corresponding positions x_{min}, $L - x_{min}$. The measure of the overlap of the two PSs is the deviation of the amplitude of CDW at $x = L/2$ from unity. Its value at the moment of PS is about 0.9.

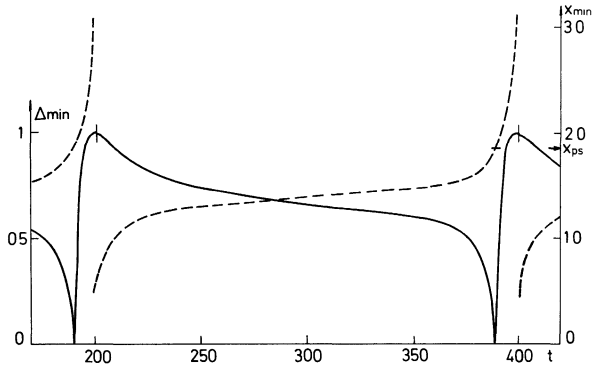

Fig. 3. — The time dependence of the minimum of CDW amplitude Δ_{min} (full line) and of its position (dashed line) for $L = 10$ and $E = 0.175$. The new cycles start consecutively at $t \simeq 200$ and $t \simeq 400$.

Figure 3 shows that the PS is a rather fast process, although the well defined but rather weak minimum in $|\Delta|$ at x_{min} is present almost all the time. Especially abrupt is the « recovery » after the PS, which is complete, i.e. $|\Delta(x)|$ returns to unity already after $\sim 0.05\, t_p$. During the PS the position x_{min} moves away fastly from the sample end. Immediately after attaining $|\Delta| \simeq 1$ all over the sample, a « seed » of the consecutive PS appears close to the sample edge, and a new cycle starts.

The time period of one cycle in figure 3 is very long compared to the characteristic reduced time scale present in (2), $2\pi/E$. In fact, the dependence of t_p on the electric field (Fig. 4) can be fitted rather well by the law

$$t_p \sim (E^2 - E_T^2)^{-1/2} \tag{16}$$

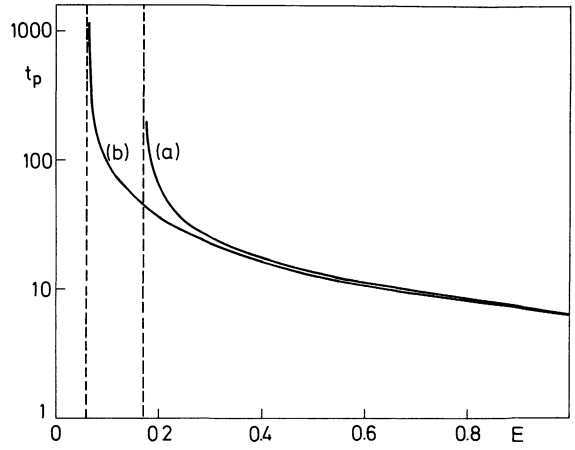

Fig. 4. — The dependence of the time period t_p on the electrical field E for sample lengths $L = 10$ (a) and $L = 20$ (b). Note the logarithmic time scale.

in the whole range of $E \geqslant E_T$, irrespectively of the value of L. This fit suggests the singular limit $E \to E_T$,

$$t_p \sim (E - E_T)^{-\beta}$$

with $\beta \simeq 0.5$. The direct estimations on the logarithmic scale with the uncertainty in values of $E_T(L)$ shown in figure 1, gave also the values of β in this range, with the precision of about 10 %. On the other hand, as $E - E_T(L)$ increases, the time period approaches the asymptotic dependence

$$t_p \simeq 2\pi/E, \tag{17}$$

which is also characteristic for semi-infinite systems, as will be seen in section 3.2.

For electrical fields smaller than $E_T(L)$, $\Delta(x)$ relaxes towards a stationary state in a time which is again longer and longer as E approaches E_T. The form of the amplitude and the phase of the stationary states is shown in figure 5a, b for a few values of $E_T - E$, and $L = 10$. As $E_T - E$ decreases, the minimum in the amplitude $|\Delta(x)|$ deepens, while the phase $\phi(x)$ becomes simultaneously more and more twisted.

By analysing the cases of small sample length (e.g. $L = 5$) we easily detected that the threshold field E_T is preceeded by the range of fields for which the relaxation to the stationary state goes through damped oscillations. The amplitude and the period of these oscillations increase as $E \to E_T$. However as L increases this oscillation range of fields preceeding E_T narrows rapidly and becomes difficult for nume-

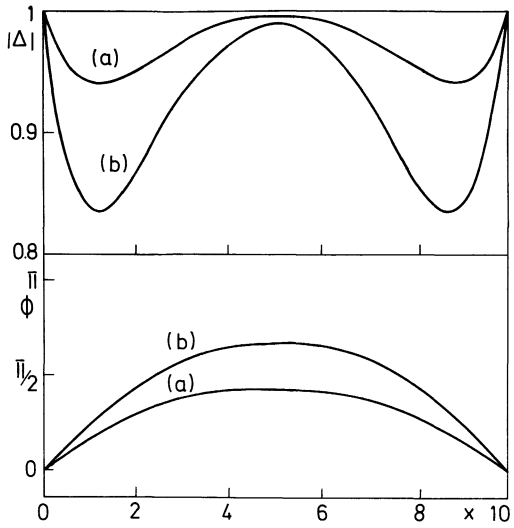

Fig. 5. — The amplitude $| \Delta(x) |$ and the phase $\phi(x)$ of the stationary solutions in the sample with $L = 10$ and for two values of electrical field ($E = 0.1$ (a) and $E = 0.15$ (b)) below the threshold field $E_T(10) \simeq 0.1722$.

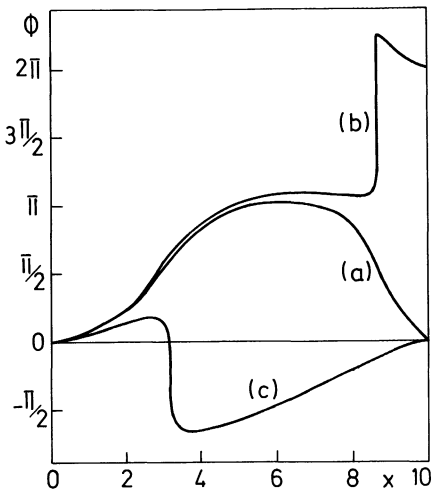

Fig. 6. — The phase $\phi(x)$ for $E = 0.225$ in the sample with $L = 10$ and asymmetric boundaries, $\Delta_0 = 3$ and $\Delta_L = 1$. The curves (a), (b) and (c) represent respectively $\phi(x)$ before any PS, after the first PS close to the right edge, and after the second PS close to the left edge.

rical analysis requiring a large amount of computer time.

The symmetry $x \leftrightarrow L - x$ present in all above results has its obvious origin in our particular choice of boundary conditions (14), by which the left ($x = 0$) and the right ($x = L$) edges of the sample are completely equivalent. It is important to discuss the effects of lifting this degeneracy. We model the fixed asymmetric boundaries by putting

$$| \Delta(x = 0, t) | = \Delta_0 , \qquad | \Delta(x = L, t) | = \Delta_L , \quad (18a)$$

and by choosing

$$\Delta(x, t = 0) = 1 + (\Delta_0 - 1)[1 - \tanh x] + \\ + (\Delta_L - 1)[1 - \tanh (L - x)] \quad (18b)$$

as the initial CDW state. As expected, PSs in a sample with $\Delta_0 \neq \Delta_L$ occur neither at the same distances from respective edges, nor in the same moment. The higher the edge amplitude, the more distant is the position of PS. The first PS occurs at a « lower » edge, it is followed by the PS on the opposite side, etc. Due to that, the basic property of PS, i.e. the jump of the overall phase difference between two edges by 2π, can be now directly seen. $\phi(x)$ for $L = 10$, $E = 0.225$, $\Delta_0 = 3$, $\Delta_L = 1$ and in different moments, is shown in figure 6. The difference $\phi(L) - \phi(0)$ is 2π after odd, and 0 after even, numbers of PSs.

The separation in time of PSs from the opposite sides does not seem to have much impact on the periodic time behaviour of $\Delta(x, t)$. We did not find any noticeable trace of e.g. double periodicity. $\Delta(x, t)$ remains a simple periodic function, at least for values of Δ_0 and Δ_L for which the slippage centres are not too close to one another. Even more, its time period, $t_p(E)$, obeys again the laws (16, 17) obtained for symmetric boundary conditions.

The same analysis also indicates that, with the increase of the CDW amplitude at the edges, the threshold field E_T increases, but rather slightly. Moreover, the shift of the curve $E_T(L)$ in the figure 1 goes without any visible change of its slope.

We thus come to the suggestion that both critical exponents, α (Eq. (15)) and β (Eq. (16)) are not affected by uncontrollable details in different sample contacts. This is particularly promising regarding the measurements of the $E_T(L)$ dependence, in which each experimental point has its own boundary conditions.

3.2 SEMI-INFINITE SYSTEMS. — The problem of a semi-infinite system with the boundary conditions given by $| \Delta(x = 0, t) | = \Delta_0$ and (10) can be analytically treated in the limit $E \gg 1$ [8]. The solution is the sum of the functions

$$\Delta_{\text{left}}(x, t) = \Delta_0 \exp[-(1 - i)\sqrt{E/2}\, x] \quad (19)$$

and

$$\Delta_{\text{right}}(x, t) = \exp[iEt] \tanh (x/\sqrt{2}), \quad (20)$$

which respectively describe the CDW close to the fixed edge ($x \lesssim 1$), and at the distant free end $x \gtrsim 1$. The matching of two behaviours gives [8]

$$x_{ps} \simeq \frac{1}{\sqrt{2E}} \ln E \quad (21)$$

(see also Eq. (9)).

Our aim was to determine how this dependence will be modified when E falls in the physically interesting range of small values. The trial ($t = 0$) function is still

taken in the form suggested by the $E \gg 1$ solution (19, 20)

$$\Delta(x, t = 0) = \Delta_0 \exp[-(1 - i)\, x/x_1] + \tanh(x/x_2), \quad (22)$$

with x_1, x_2 treated as variational parameters. We then followed numerically the evolution of this function in time. The range of investigated fields went from $E = 10$ down to $E = 10^{-2}$. The scheme of this analysis is shown in figure 7, where the position of the PS is plotted as a function of the field E for $\Delta_0 = 1$. While the results for fields $E \gtrsim 1$ reproduce well the analytical result (21), the range of small fields $E \leqslant 1$ is characterised by the power law

$$x_{ps}(E) \simeq 1.15\, E^{-\gamma}. \quad (23)$$

with $\gamma = 0.284 \pm 0.004$.

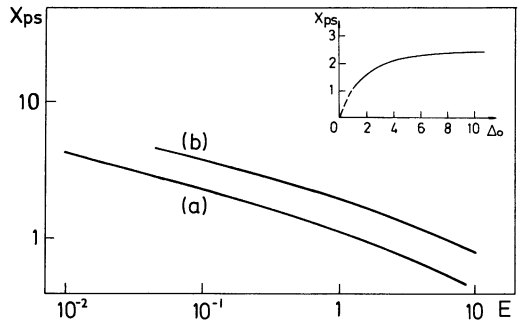

Fig. 7. — The distance of the PS-centre from the fixed end, x_{ps}, as a function of the elctrical field for $\Delta_0 = 1$ (a) and $\Delta_0 = 3$ (b). The insert shows the dependence of x_{ps} on Δ_0 for $E = 1$.

The time and space dependence of $\Delta(x, t)$ in the slippage part of x-space is equivalent to that obtained for slippages in long finite samples (Figs. 3, 6). As E decreases the process of PS becomes more and more rapid on both, x and t, scales. Simultaneously x_{ps} increases (Fig. 7). In the numerical computation this means that we have to increase both, the density of discrete x-points and the length L_∞, which makes the analysis of fields weaker than $E \approx 10^{-2}$ hardly accessible.

As in the case of finite samples, the above results are not very sensitive to the value of amplitude at the fixed end, Δ_0. Higher values of Δ_0 lead to the shift of x_{ps} towards the free end (see the curve $x_{ps}(E)$ for $\Delta_0 = 3$ in Fig. 7). This shift saturates as Δ_0 increases, as is shown in the insert of figure 7. The change of Δ_0 does not affect the exponent γ in equation (23) and the time period, t_p. The latter is equal to $2\pi/E$ in the whole investigated range of fields E and amplitudes at the fixed end, Δ_0.

All numerical solutions considered until now have one common property, namely that after some amount of time needed for the stabilization they show a simple periodic behaviour, with $\Delta(x, t)$ being the one-periodic function. In other words, the PSs, when they exist, always occur at the same positions on the x-scale and in the equidistant time intervals. The important question which arises regarding this point is whether (2) has some other, possibly multiperiodic, limit cycles as its solutions. If such a limit cycle exists, there should be some set of initial functions $\Delta(x, t = 0)$ associated with it. In order to find out whether such a set exists among the functions (22), we varied the parameters x_1 and x_2 in wide ranges of values, but always got the stabilization to the described limit cycle, usually after times which are of the order of, or shorter than, the period t_p. The same happened in the case of finite samples for initial functions which were chosen to have a finite number of loops ($\phi(L) - \phi(0) = 2\pi n$ at $t = 0$). Before attaining the limit cycle, these functions lost all loops in a sequence of n PSs, and then continued to behave like solutions of section 3.1.

Another type of initial functions which we investigated is that suggested by (6). For $E \lesssim 1$ these functions are unstable in a wide range of x-values, if the linearized version of (2) is used. However, when the nonlinearity is retained, the time evolution brings fastly again these functions to the limit cycle considered in this section. Thus, all our attempts to find some other limit cycle were unsuccessful. The suggestion of this analysis is that (2) has very probably only one, simple periodic, limit cycle which has been described in this section.

3.3 THE VOLTAGE ORIGINATING FROM PHASE SLIPPAGES. — The PSs are the kind of edge phenomena which do not affect the interior of long ideal samples. The CDW in the interior of sample has the simple sinusoidal form (10). The corresponding voltage along the sample is constant in time and scales with the length of the sample.

The sequence of PSs through which the CDW passes close to the sample contacts has on the contrary a highly nonsinusoidal time dependence, and therefore leads to a finite time dependent voltage $V(t)$ (13), usually called the periodic noise. Apparently, the time period for $V(t)$ is determined by the time behaviour of PS-solutions given in figures 3 and 4. Thus, for semi-infinite sample and for finite sample with $E - E_T(L) \gg E_T(L)$, the fundamental frequency ν_f in the Fourier spectrum of $V(t)$ is equal to $E/2\pi$ in our dimensionless notations.

The function $V(t)$ for the semi-infinite system and for a few values of the electric field E is shown in figure 8. (In this and all subsequent figures the voltage is divided by λ, and is plotted in the reduced unit defined in section 2. The parameter ε in equations (3) and (11) is for simplicity chosen equal to unity). $V(t)$ raises steeply in short time intervals in which PSs occur, and has the overall form of asymmetric and rather broad pulses. These pulses which are present in a wide range of values of E, become more pronounced as E decreases.

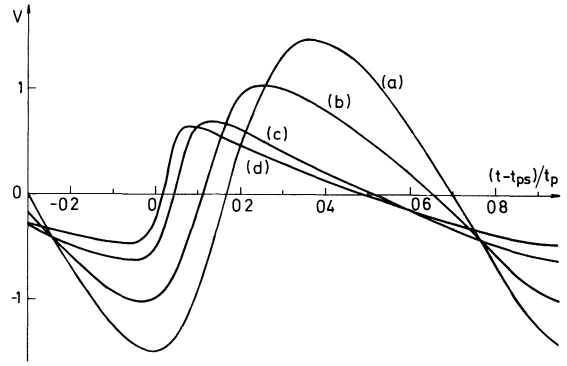

Fig. 8. — The voltage V *vs.* t/t_p in the semi-infinite system with $\Delta_0 = 1$ and for the electrical fields $E = 1.0$ (a), 0.5 (b), 0.2 (c) and 0.13 (d). The PS occurs at t_{ps}.

The strength of the voltage $V(t)$ increases with E as is directly seen in figure 8. This increase can be followed more quantitatively by calculating the amplitude of the first harmonic of $V(t)$,

$$V_1 = \left| t_p^{-1} \int V(t) \exp(i\, 2\, \pi \nu_f\, t)\, dt \right| . \qquad (24)$$

The result is shown in figure 9, again for the semi-infinite system. In the range of weak electric fields ($E \lesssim 1$) we get

$$V_1 \simeq 1.5\, E^{\delta}, \qquad (25)$$

with $\delta = 0.56 \pm 0.02$. The behaviour (25) of V_1 differs thus from the behaviour of $Ex_{ps}(E) \sim E^{0.72}$. In other words, the characteristic x scale of nonlinear PS diffusion depends on E in a way which differs somewhat from the law obeyed by $x_{ps}(E)$.

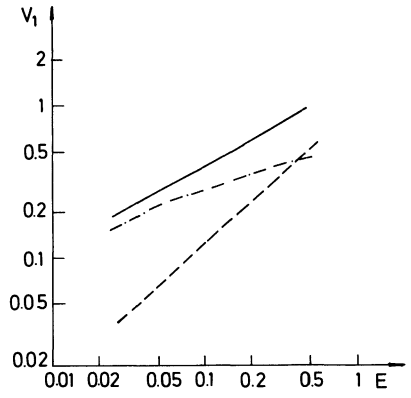

Fig. 9. — The amplitude of the first harmonic of the voltage, V_1 (full line), *vs.* the electrical field E. The two contributions proportional to $|\Delta|^2 E$ and $|\Delta|^2 \dot{\phi}$ (Eq. (11)) are shown by the dashed and dashed-dotted lines respectively.

The voltage $V(t)$ is the sum of two terms, proportional to $|\Delta|^2 E$ and $|\Delta|^2 \dot{\phi}$ (see Eqs. (3) and (11)). The corresponding decomposition of V_1 in figure 9 shows that the later, $\dot{\phi}$-dependent term becomes relatively more and more dominant as the electrical field E decreases. This is also seen in figure 10, in which the two contributions are plotted on the time scale for $E = 0.13$. The term $|\Delta|^2 \dot{\phi}$ not only dominates over the term $|\Delta|^2 E$, but also varies more dramatically during the PS process.

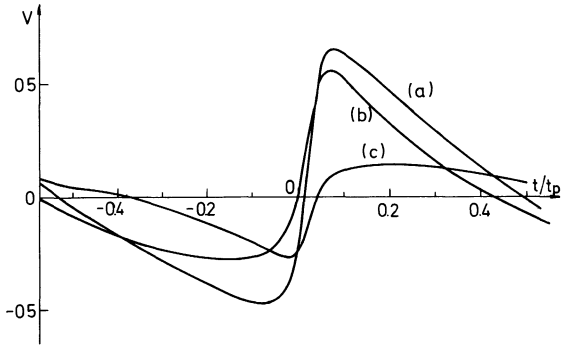

Fig. 10. — The voltage $V(t)$ (curve (a)) for $E = 0.13$ and $\Delta_0 = 1$, decomposed into $|\Delta|^2 \dot{\phi}$ (b) and $|\Delta|^2 E$ (c) contributions (see Eq. (11)).

The voltage $V(t)$ of finite samples has properties similar to those presented in figure 8. It still significantly deviates from the sinusoidal form even for $E \gg E_T(L)$ (Fig. 11). In the limit $E \to E_T(L)$ the pulses become markedly sharp and narrow. For asymmetric boundary conditions ($\Delta_0 \neq \Delta_L$), when PSs at the opposite edges of the sample do not coincide in time, $V(t)$ may show two distinct and nonequivalent pulses per period. Some of the examples are shown in figure 12.

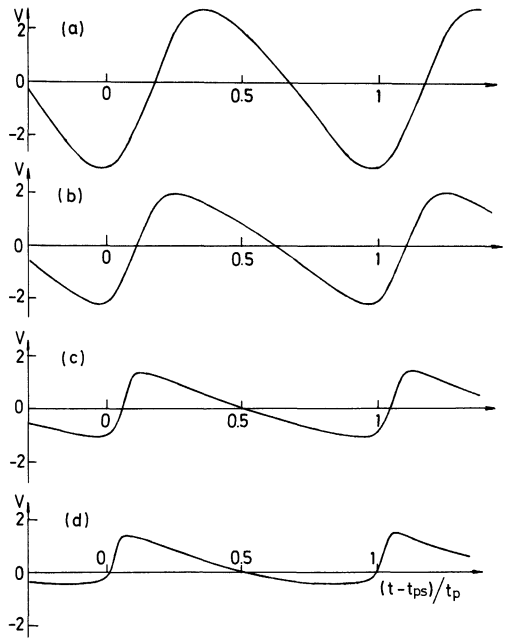

Fig. 11. — The voltage V *vs.* t/t_p in the finite sample ($L = 15$) with symmetrical edges ($\Delta_0 = \Delta_L = 1$), and for the electrical fields $E = 1.0$ (a), 0.5 (b), 0.2 (c) and 0.1 (d). The threshold field is $\simeq 0.094$.

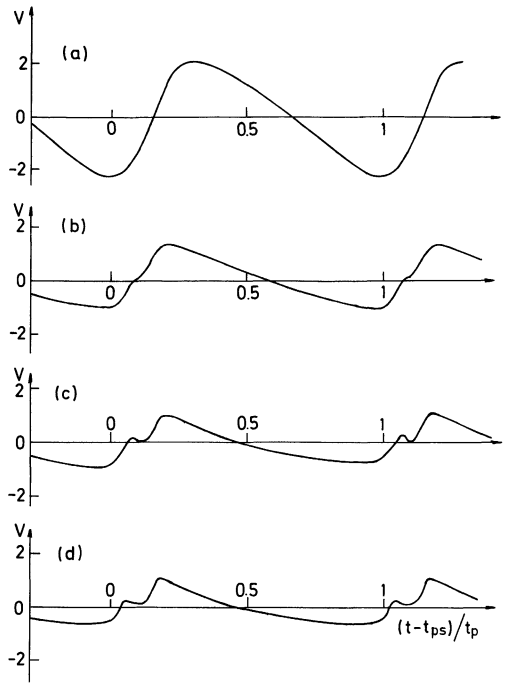

Fig. 12. — The voltage $V(t)$ in the finite sample ($L = 15$) with asymmetric edges ($\Delta_0 = 3$, $\Delta_L = 1$), and for the electrical fields $E = 0.5$ (a), 0.2 (b), 0.15 (c) and 0.13 (d).

4. Discussion and conclusions.

We have shown that the PS process is a strongly nonlinear phenomenon. Our numerical results from section 3 show that none of the expected α's in the behaviour $x_{ps} \sim E^{-\alpha}$ mentioned in section 2 is realized. Instead we have got $\alpha \simeq 0.28$, i.e. an even stronger restriction on the distance of PS from the interface than that suggested by (9). However we have not numerically reached the range of very weak fields (our lowest values for E were $\sim 10^{-2}$), so that we cannot completely exclude the possibility that the regime defined by results (15) and (23) is changed for lower values of E. Still, we hope that these results could be considered as relevant for the interpretation of some experiments.

Our result for $E_T(L)$ suggests that the threshold field increases on decreasing the length of the sample. Such behaviour was reported in works on $NbSe_3$ [13] and orthorhombic TaS_3 [14]. The experimental range of sample lengths was about $L \simeq 10^3$-10^4 (down to ~ 20 μm in $NbSe_3$ and ~ 60 μm in TaS_3). Caution is required in fitting these data due to the experimental technique used in reference [14] and to the properties of contacts which are far from ideal in shape and in dimension [13-15]. Furthermore, threshold fields associated with contacts are not very much larger than the bulk ($L \to \infty$) threshold fields. Nevertheless, after subtracting the bulk threshold field E_{tb}, a preliminary comparison shows that (15) gives a good estimate of the observed values of $E_T(L)$. The experimental $E_T(L)$ dependence can be well fitted with the exponent α. For a more detailed test of the present results, a further careful investigation of the role of particular contacts is desirable. In this respect it is encouraging that the most important results of this work are insensitive to those variations in our idealized boundary conditions which were considered in section 3.

The characteristics of periodic voltage which originates from PS processes are clearly in qualitative agreement with the considered experimental findings. The experiments of Gill [5] and of Ong and Verma [6] showed that the oscillations in $V(t)$ are localized close to the interfaces (i.e. to the contacts), and that $V(t)$ is independent of the length of the sample. Ong and Verma [5] identified the number of fundamental frequencies in the periodic noise [16] with the number of segments into which the sample is divided due to the presence of contacts. Thus, with two contacts at its edges, and two contacts in between, the sample presents a series of three disconnected segments. The reason for differences among frequencies belonging to different segments may be attributed to the different values of local electric fields established in each segment. This is in agreement with the observed effects of shunting the segments [6], and with the fact that the fundamental frequencies approach each other when the external electric field increases [16] so that the relative difference among local fields is suppressed. Still, we note that the division into segments is perhaps not complete in the sense that the CDWs from the opposite sides of a contact are fully independent, so that boundary conditions which are more realistic than those used in our analysis, could be needed.

The fundamental frequency of the voltage $V(t)$ is for $E \gg E_T(L)$ proportional to the external electric field, with the slope given in dimensional variables by

$$v_f = \frac{16\,\gamma}{9\,\pi^2}\,\frac{\xi_0\,e}{\hbar}\,E\,.$$

This value of the slope is of the order of experimental values measured e.g. in $NbSe_3$ [16]. The multiharmonic nature of the periodic noise obtained in these experiments is also present in our result (Figs. 8, 10-12). A more detailed harmonic analysis of these results is in progress. We point out that the amplitude of e.g. the first harmonic of $V(t)$, given by (25) and figure 9 reproduces well the actual $V_1(E)$ dependence in some samples of $NbSe_3$ [16].

We finally note that more experimental and theoretical work is needed for the understanding of the $v_f(E)$ behaviour in the range of fields $E \to E_T(L)$. Result [16] could be applicable for short samples (or segments), for which $E_T(L) \gg E_{tb}$. Dynamical measurements of this type are highly desirable. The known dynamical data [1, 2, 16] are obtained on long samples with $E_T \simeq E_{tb}$, in which the noise from PSs could be strongly correlated with the pinning processes in the bulk. This situation, as well as the process of PSs in the time alternating external electric fields will be subject to further investigations.

To summarize, we have shown that (2) based on a rather simplified microscopic model predicts a number of interesting new phenomena and demonstrates the richness of the nonlinear processes responsible for the conversion of the collective current transported by the Fröhlich mode motion into the ordinary conducting mechanism at the boundary between two metals.

Acknowledgments.

The authors are grateful to S. Barišić for useful discussions and careful reading of the manuscript, and to P. Monceau for correspondence and helpful suggestions. One of us (L.P.G.) thanks for hospitality during his visit to the University of Zagreb.

References

[1] FLEMING, R. M. and GRIMES, G. G., *Phys. Rev. Lett.* **42** (1979) 1423.

[2] MONCEAU, P., RICHARD, J. and RENARD, M., *Phys. Rev. Lett.* **45** (1980) 43 ; *Phys. Rev. B* **25** (1982) 931.

[3] ZETTL, A., GRÜNER, G. and THOMPSON, A. H., *Phys. Rev. B* **26** (1982) 5760 ;
ZETTL, A., JACKSON, C. M. and GRÜNER, G., *Phys. Rev. B* **26** (1982) 5773.

[4] Colloque International du CNRS sur la Physique et la Chimie des Métaux Synthétiques et Organiques, Les Arcs 1982, *J. Physique Colloq.* **44** (1983) C3, ed. R. Comès, P. Bernier et J. Rouxel.

[5] GILL, J. C., *Solid State Commun.* **44** (1982) 1041.

[6] ONG, N. P. and VERMA, G., *Phys. Rev. B* **27** (1983) 4495.

[7] ONG, N. P., VERMA, G. and MAKI, K., preprint (1983).

[8] GOR'KOV, L. P., *Pis'ma Zh. Eksp. Teor. Fiz.* **38** (1983) 76.

[9] GOR'KOV, L. P., *Zh. Eksp. Teor. Fiz.*, in press (1983).

[10] HOROWITZ, B., GUTFREUND, H. and WEGER, M., *Solid State Commun.* **39** (1981) 541.

[11] KEL'DISH, L. V. and KOPAEV, Yu. V., *Fiz. Tverd. Tela* **6** (1964) 2791.

[12] FUNG, K. K. and STEEDS, J. W., *Phys. Rev. Lett.* **45** (1980) 1696.

[13] SAINT-LAGER, M. C., Thèse, Grenoble 1983.

[14] MIHÁLY, G., HUTIRAY, Gy. and MIHÁLY, L., *Phys. Rev. B* **28** (1983) 4896.

[15] MONCEAU, P., private communication.

[16] RICHARD, J., MONCEAU, P. and RENARD, M., *Phys. Rev. B* **25** (1982) 948.